Exploring the potential for Active Galactic Nuclei (AGN) emission line delays using LSST

Swayamtrupta Panda

[1]CNPq/PCI Fellow, Laboratorio Nacional de Astrofisica, Itajubá - MG, Brazil
[2]Science Team Member, AGN-DESC-TVS Science Collaborations
[3]Data Preview Delegate

spanda@lna.br

Outline

- AGN variability and Reverberation Mapping
- Vera Rubin Observatory's LSST and AGN census
- Our pipeline (results and progress)

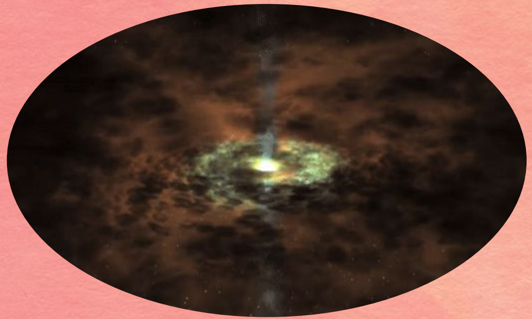

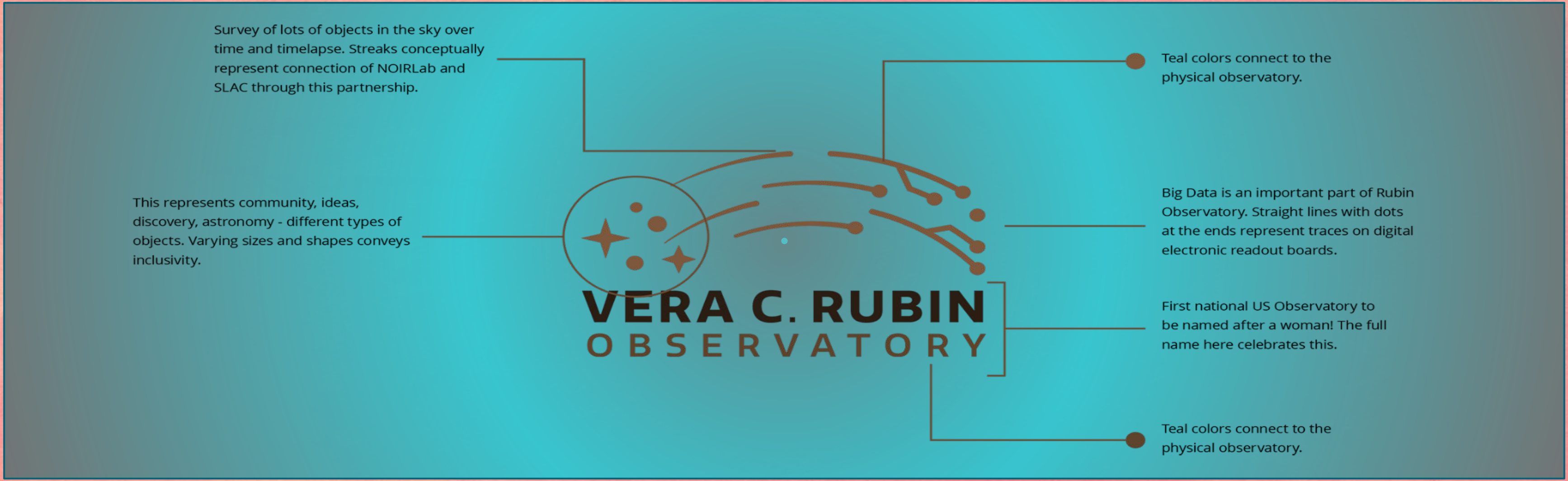

SOME PHYSICS

Reverberation Mapping

Given a velocity and a distance, we can use Kepler's laws to tell us the BH mass!

$$M_{\mathrm{BH}} = f\,\frac{r_{\mathrm{BLR}}\mathrm{FWHM}^2}{G}$$

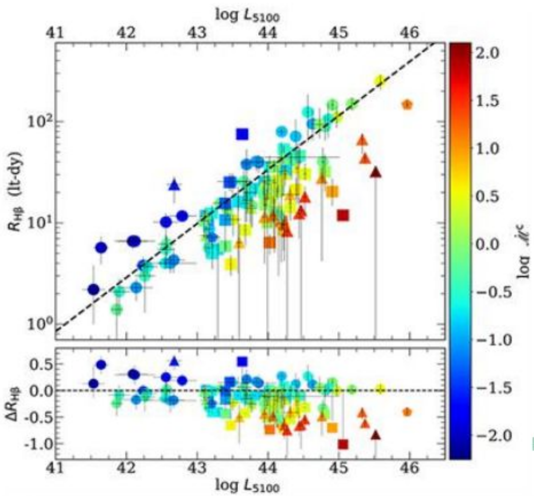

Panda et al. (2019)

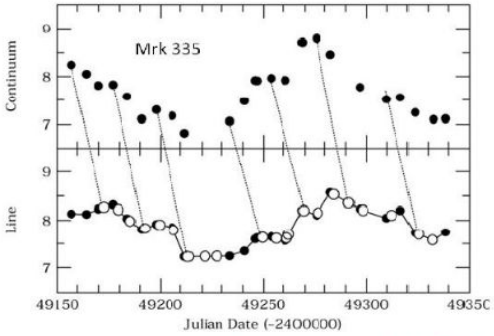

Peterson et al. (2001)

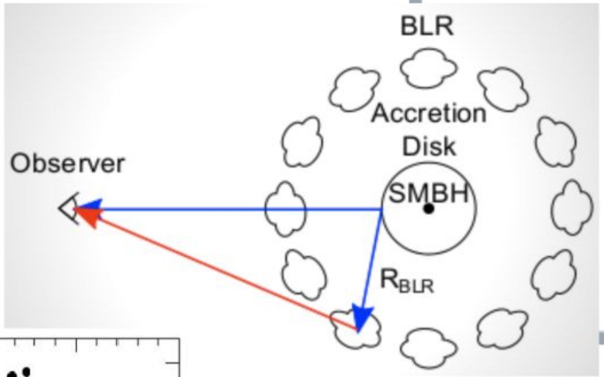

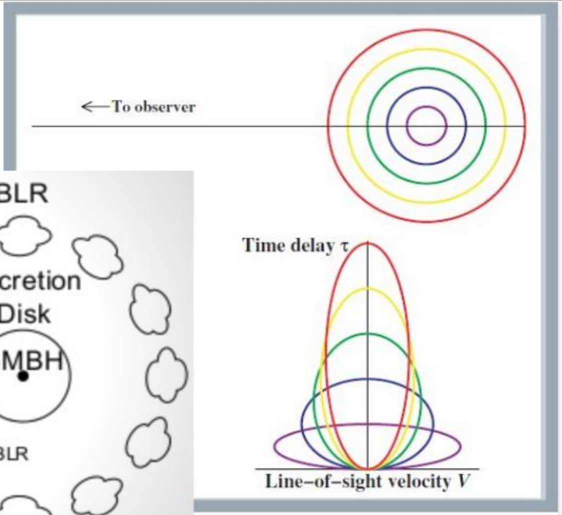

Reverberation mapping relies on the fact that the light emitted by the BLR is reprocessed from the central continuum source, and that the central continuum source is variable

SOME PHYSICS

Reverberation Mapping

Given a velocity and a distance, we can use Kepler's laws to tell us the BH mass!

$$M_{\mathrm{BH}} = f\,\frac{r_{\mathrm{BLR}}\mathrm{FWHM}^2}{G}$$

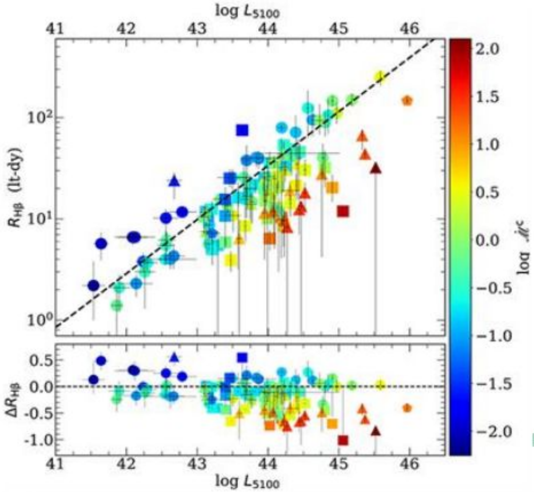

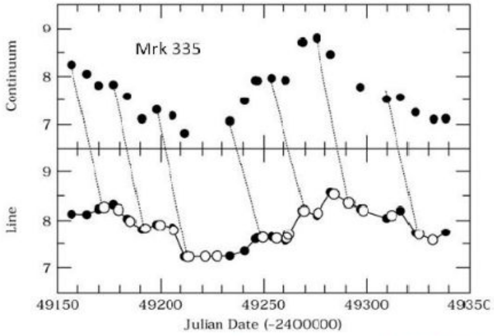

Peterson et al. (2001)

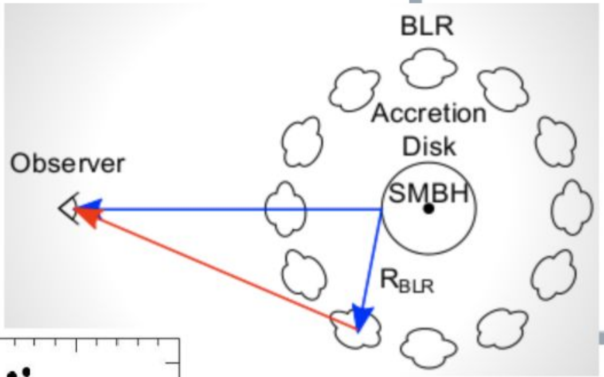

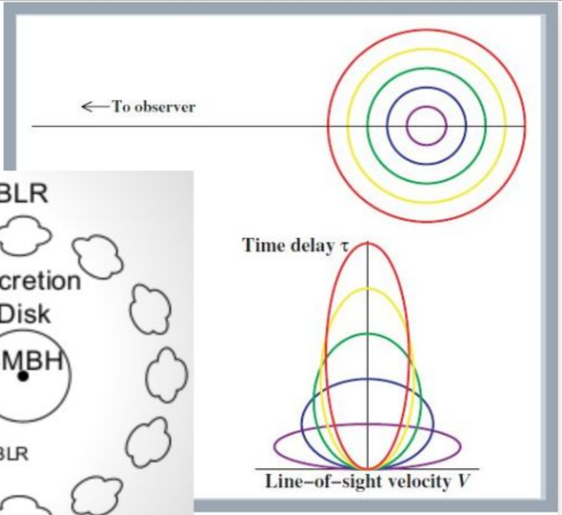

Reverberation mapping relies on the fact that the light emitted by the BLR is reprocessed from the central continuum source, and that the central continuum source is variable

We have > 200 RM AGNs now with Hβ-emitting BLR sizes!

Local Universe → Quasars → Early Universe

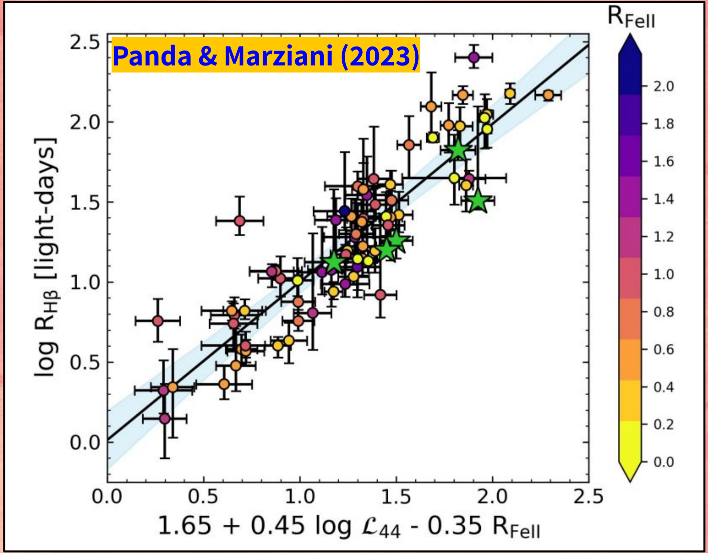

$$\log\left(\frac{\mathrm{R_{BLR}}}{1\ \mathrm{light-day}}\right) = \kappa + \alpha \log\left(\frac{\mathrm{L_{5100}}}{10^{44}\ \mathrm{erg\ s^{-1}}}\right) + \gamma \mathrm{R_{FeII}}$$

Reverberation – mapping
+
single – epoch spectroscopy

$$\mathrm{D_L} = \sqrt{\mathrm{L_{5100}}/4\pi \mathrm{F}} \propto \frac{c\tau}{\sqrt{4\pi F}}$$

Local Universe → Quasars → Early Universe

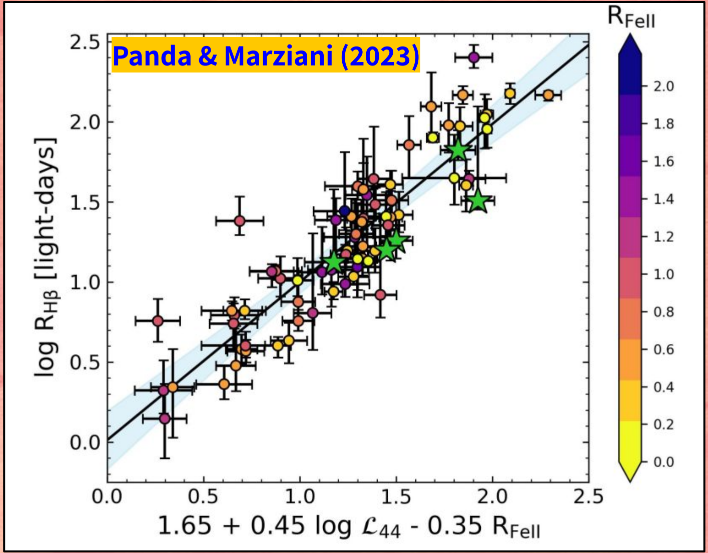

$$\log\left(\frac{R_{BLR}}{1\ \mathrm{light-day}}\right) = \kappa + \alpha \log\left(\frac{L_{5100}}{10^{44}\ \mathrm{erg\ s^{-1}}}\right) + \gamma R_{FeII}$$

Reverberation – mapping
+
single – epoch spectroscopy

$$D_L = \sqrt{L_{5100}/4\pi F} \propto \frac{c\tau}{\sqrt{4\pi F}}$$

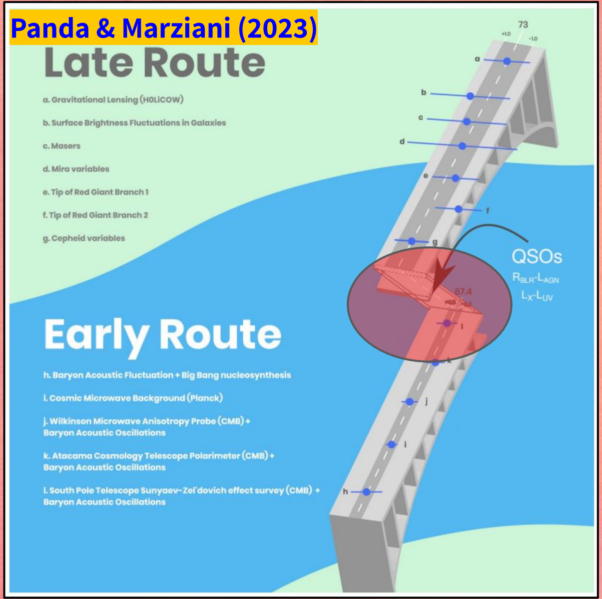

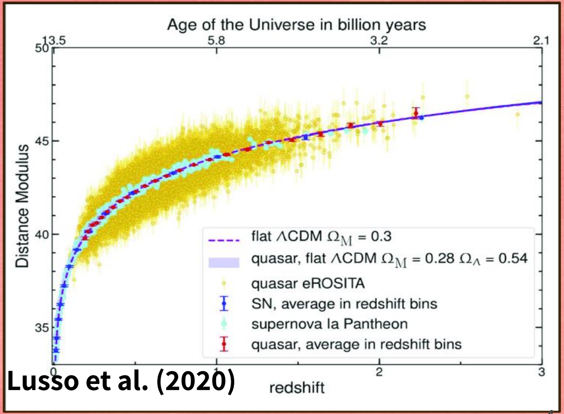

The Vera C. Rubin Observatory

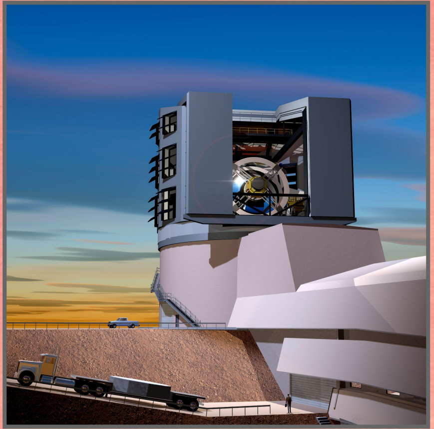

The goal of the Vera C. Rubin Observatory project is to conduct the **10-year Legacy Survey of Space and Time (LSST)**. LSST will deliver a 500 petabyte set of images and data products - create a decade-long movie of our Universe, that will address some of the most pressing questions about the structure and evolution of the universe accounting for tens of millions of AGNs (z ≳ 7).

The 8.4-meter Simonyi Survey Telescope uses a special three-mirror design, which creates an exceptionally wide field of view, and has the ability to **survey the entire sky in only three nights**.

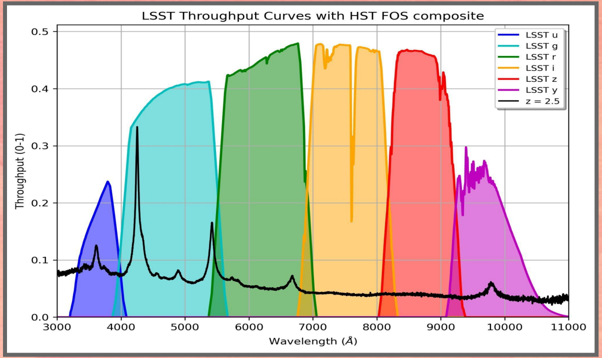

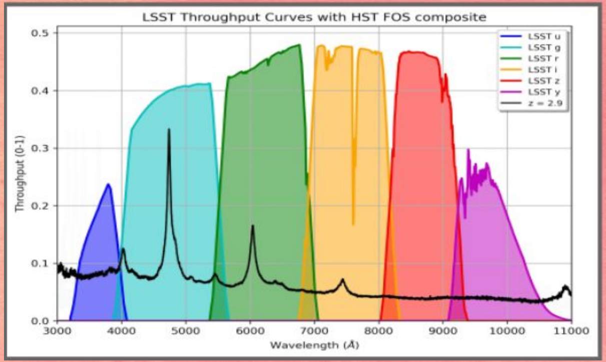

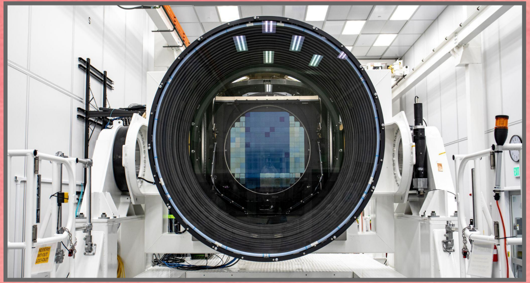

3200 Megapixel camera

Photo-RM with VRO-LSST

Panda et al. (2019)

Modeling AGN Variability, making predictions

We are developing a pipeline for time delay measurements in LSST photometric channels that can measure the **emission line time delays for any quasar detected by Vera Rubin Observatory** from any part of the observable sky; incorporated the **latest suite of cadence simulations** and assess them based on the success rate of lag recovery

- ***Analysis with real light curves (spectro-photometric reverberation mapping using SALT, etc.)***
- ***Time-delay measurements***
- ***Efficient analyses accounting for the contamination from the starlight and other emission lines***
- ***Incorporating distribution of widths for realistic black hole mass distribution, line widths***
- ***Improving the prediction quality, testing on the DDF fields***

Modeling AGN Variability, making predictions

We are developing a pipeline for time delay measurements in LSST photometric channels that can measure the **emission line time delays for any quasar detected by Vera Rubin Observatory** from any part of the observable sky; incorporated the **latest suite of cadence simulations** and assess them based on the success rate of lag recovery

- ***Analysis with real light curves (spectro-photometric reverberation mapping using SALT, etc.)*** ✅
- ***Time-delay measurements*** ✅
- ***Efficient analyses accounting for the contamination from the starlight and other emission lines*** ✅
- ***Incorporating distribution of widths for realistic black hole mass distribution, line widths*** ✅
- ***Improving the prediction quality, testing on the DDF fields*** ✅

Modeling AGN Variability, making predictions

We are developing a pipeline for time delay measurements in LSST photometric channels that can measure the **emission line time delays for any quasar detected by Vera Rubin Observatory** from any part of the observable sky; incorporated the **latest suite of cadence simulations** and assess them based on the success rate of lag recovery

- ***Analysis with real light curves (spectro-photometric reverberation mapping using SALT, etc.)*** ✅
- ***Time-delay measurements*** ✅
- ***Efficient analyses accounting for the contamination from the starlight and other emission lines*** ✅
- ***Incorporating distribution of widths for realistic black hole mass distribution, line widths*** ✅
- ***Improving the prediction quality, testing on the DDF fields*** ✅

Producing mock light-curves

- *Campaign duration (10 years)*
- *Number of visits per photometric band*
- *Photometric accuracy*
- *black hole mass distribution*
- *Line EWs and FWHMs from the latest SDSS Quasar Catalogue (DR16)*
- *Emission lines contamination folded with theoretical light-curves using power spectral distribution and Timmer-Koenig algorithm (with red noise properties typical of quasars)*
- *Pairs of channels with uniform and variable time distributions*
- *Time delay estimation using standard radius-luminosity relation*

Representative light-curves from OpSim runs

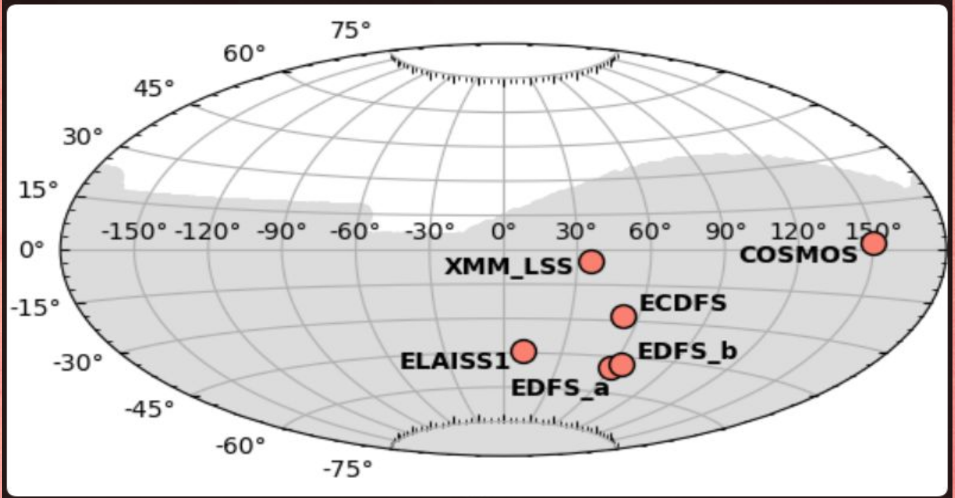

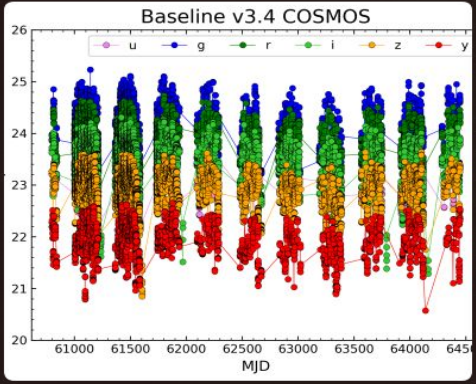

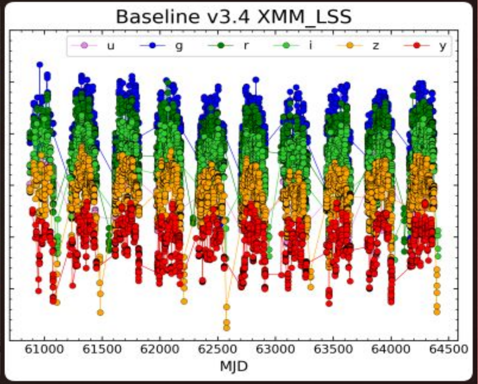

OpSim Run: <u>*ddf_baseline_v3.4_v3.4_10yrs*</u>

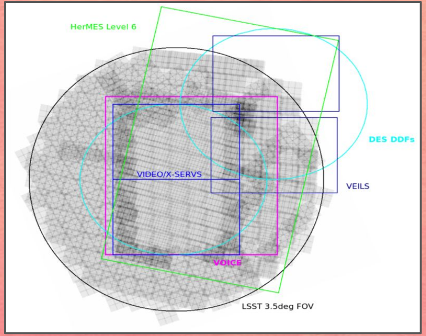

ELAIS-S1 DDF

RA=00:37:48,

Dec=-44:01:30

# of visits in 10 years:

u → 898

g → 2448

r → 4859

i → 4876

z → 5729

y → 2748

Panda et al. (2019); Czerny, Panda, et al. (2023)

Czerny, Panda, et al. (2023)

Predictions for LSST: BLR time-lag vs. AGN luminosity

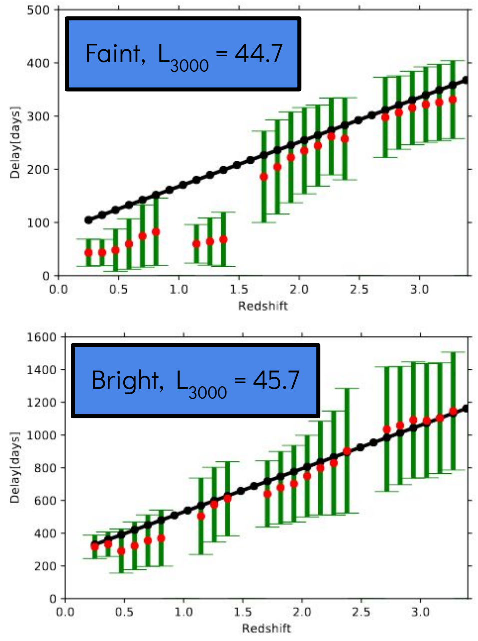

Fig. 6. The adopted and recovered time delay as a function of redshift for faint AGN ($\log L_{3000}$ = 44.7 erg s^{-1}, upper panel) and for bright AGN ($\log L_{3000}$ = 45.7 erg s^{-1}, lower panel) from 10 years of observations in the DDF. Other parameters have standard values given in Table 1.

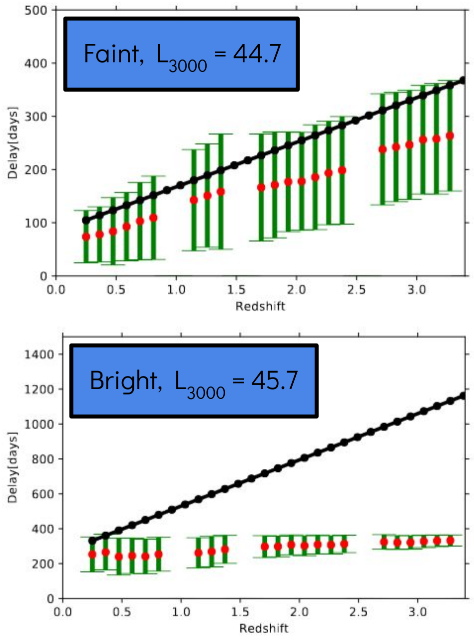

Fig. 7. The adopted and recovered time delay as a function of redshift for faint AGN ($\log L_{3000}$ = 44.7 erg s^{-1}, upper panel) and for bright AGN ($\log L_{3000}$ = 45.7 erg s^{-1}, lower panel) from 2 years of observations in the DDF. Other parameters have standard values given in Table 1.

Czerny, Panda, et al. (2023)

Predictions for LSST: BLR time-lag vs. AGN luminosity

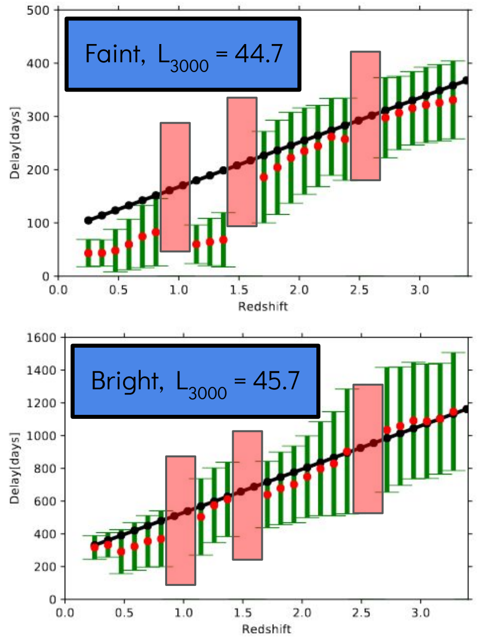

Fig. 6. The adopted and recovered time delay as a function of redshift for faint AGN ($\log L_{3000}$ = 44.7 erg s^{-1}, upper panel) and for bright AGN ($\log L_{3000}$ = 45.7 erg s^{-1}, lower panel) from 10 years of observations in the DDF. Other parameters have standard values given in Table 1.

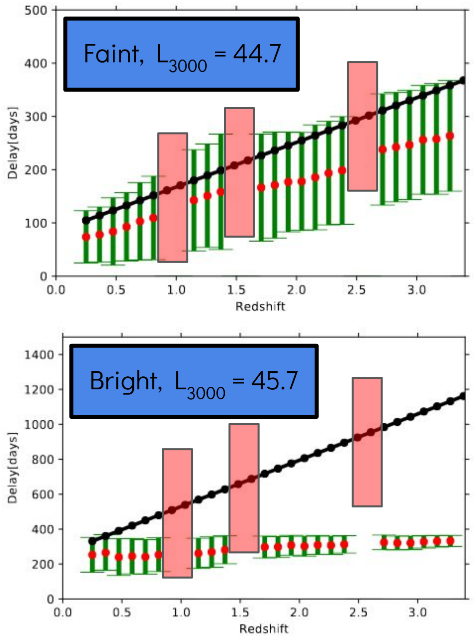

Fig. 7. The adopted and recovered time delay as a function of redshift for faint AGN ($\log L_{3000}$ = 44.7 erg s^{-1}, upper panel) and for bright AGN ($\log L_{3000}$ = 45.7 erg s^{-1}, lower panel) from 2 years of observations in the DDF. Other parameters have standard values given in Table 1.

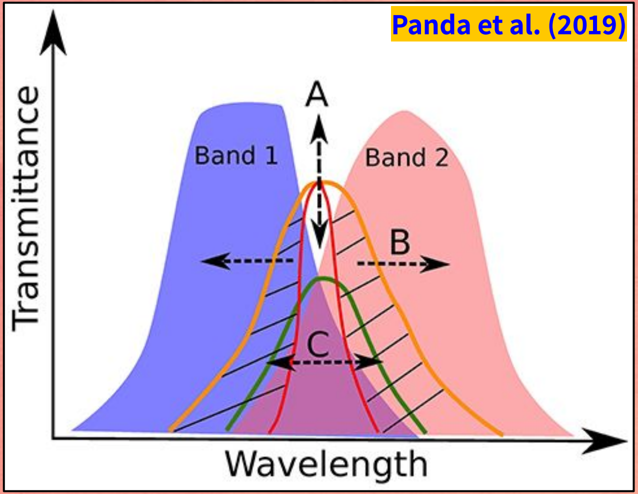

Czerny, Panda, et al. (2023)

Predictions for LSST: BLR time-lag vs. AGN luminosity

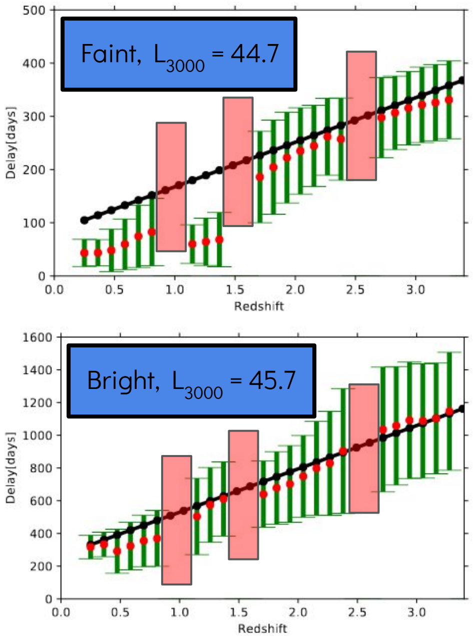

Fig. 6. The adopted and recovered time delay as a function of redshift for faint AGN ($\log L_{3000}$ = 44.7 erg s^{-1}, upper panel) and for bright AGN ($\log L_{3000}$ = 45.7 erg s^{-1}, lower panel) from 10 years of observations in the DDF. Other parameters have standard values given in Table 1.

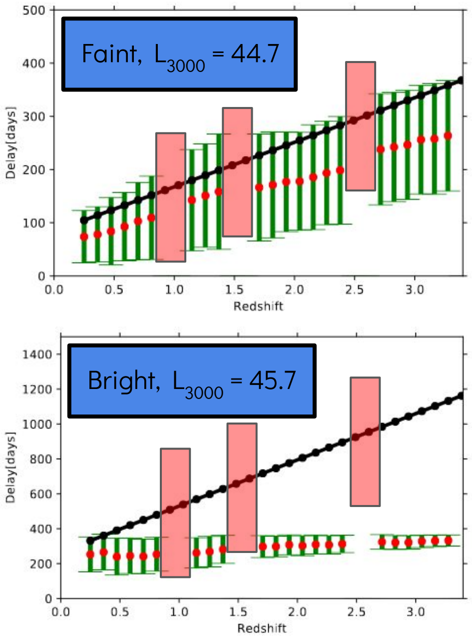

Fig. 7. The adopted and recovered time delay as a function of redshift for faint AGN ($\log L_{3000}$ = 44.7 erg s^{-1}, upper panel) and for bright AGN ($\log L_{3000}$ = 45.7 erg s^{-1}, lower panel) from 2 years of observations in the DDF. Other parameters have standard values given in Table 1.

Table 3. The effective mean separation in the observing dates in *r* band and the redshift-averaged offset of the mean recovered time delay in comparison to the assumed time delay for bright quasars, 10 years of data

Cadence	formal name	effective separation [days]	offset in delay [%]
S1-MS	baseline_v2.0_10yrs	13.7	11.7
S2-MS	baseline_v2.1_10yrs	12.4	10.0
S3-MS	baseline_v2.2_10yrs	16.0	12.8
S4-MS	draft_connected_v2.99_10yrs	16.6	10.2
S5-MS	draft_v2.99_10yrs	16.2	11.9
S6-MS	light_roll_v2.99_10yrs	13.3	11.1
S7-MS	retro_baseline_v2.0_10yrs	9.4	7.2
S8-MS	roll_early_v2.99_10yrs	15.8	11.1
S1-DDF	ddf_accourd_sf0.30_lsf0.4_lsr0.5_v2.1_10yrs	5.8	8
S2-DDF	ddf_bright_slf0.35_v2.1_10yrs	5.0	12
S3-DDF	ddf_double_slf0.35_v2.1_10yrs	3.2	16
S4-DDF	ddf_old_rot_slf0.35_v2.1_10yrs	5.0	13
S5-DDF	ddf_quad_slf0.35_v2.1_10yrs	2.7	10
S6-DDF	ddf_quad_subfilter_slf0.35_v2.1_10yrs	3.3	10
S7-DDF	ddf_season_length_slf0.20_v2.1_10yrs	5.9	10
S8-DDF	ddf_season_length_slf0.35_v2.1_10yrs	4.7	11
S2-DDF-equal	-	1.0	11.1

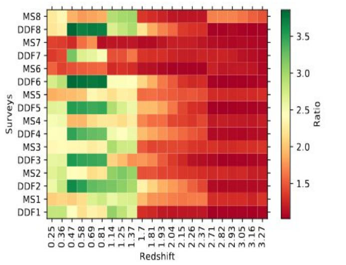

Faint, L_{3000} = 44.7

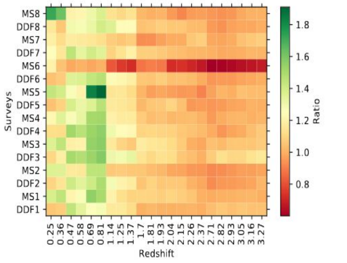

Bright, L_{3000} = 45.7

Czerny, Panda, et al. (2023)

Predictions for LSST: BLR time-lag vs. AGN luminosity

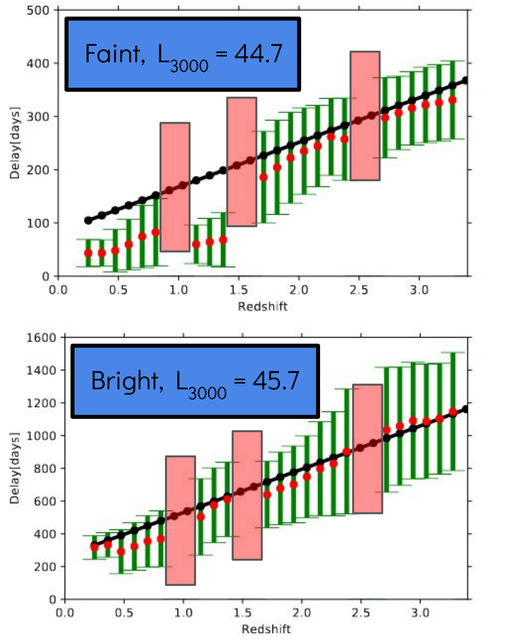

Fig. 6. The adopted and recovered time delay as a function of redshift for faint AGN ($\log L_{3000}$ = 44.7 erg s^{-1}, upper panel) and for bright AGN ($\log L_{3000}$ = 45.7 erg s^{-1}, lower panel) from 10 years of observations in the DDF. Other parameters have standard values given in Table 1.

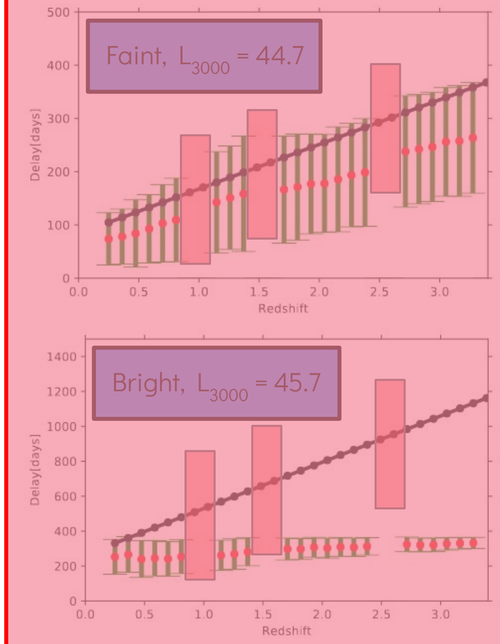

Fig. 7. The adopted and recovered time delay as a function of redshift for faint AGN ($\log L_{3000}$ = 44.7 erg s^{-1}, upper panel) and for bright AGN ($\log L_{3000}$ = 45.7 erg s^{-1}, lower panel) from 2 years of observations in the DDF. Other parameters have standard values given in Table 1.

Table 3. The effective mean separation in the observing dates in *r* band and the redshift-averaged offset of the mean recovered time delay in comparison to the assumed time delay for bright quasars, 10 years of data

Cadence	formal name	effective separation [days]	offset in delay [%]
S1-MS	baseline_v2.0_10yrs	13.7	11.7
S[illegible]	[illegible]	[illegible]	[illegible].0
S[illegible]	[illegible]	[illegible]	[illegible].8
S[illegible]	[illegible]	[illegible]	[illegible].2
S[illegible]	[illegible]	[illegible]	[illegible].9
S[illegible]	[illegible]	[illegible]	[illegible].1
S[illegible]	[illegible]	[illegible]	[illegible].2
S[illegible]	[illegible]	[illegible]	[illegible].1
S[illegible]	[illegible]	[illegible]	[illegible]3
S[illegible]	[illegible]	[illegible]	[illegible]2
S[illegible]	[illegible]	[illegible]	[illegible]6
S4-DDF	ddf_old_rot_slf0.35_v2.1_10yrs	5.0	13
S5-DDF	ddf_quad_slf0.35_v2.1_10yrs	2.7	10
S6-DDF	ddf_quad_subfilter_slf0.35_v2.1_10yrs	3.3	10
S7-DDF	ddf_season_length_slf0.20_v2.1_10yrs	5.9	10
S8-DDF	ddf_season_length_slf0.35_v2.1_10yrs	4.7	11
S2-DDF-equal	-	1.0	11.1

Dual purpose deliverable software

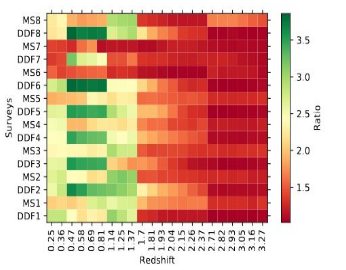

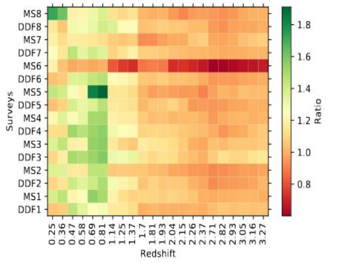

Faint, L_{3000} = 44.7

Bright, L_{3000} = 45.7

Real light curves from ZTF - testing with bonafide RM AGNs

SP, Czerny & Pozo-Nuñez (in prep.)

Wang et al. (2023)

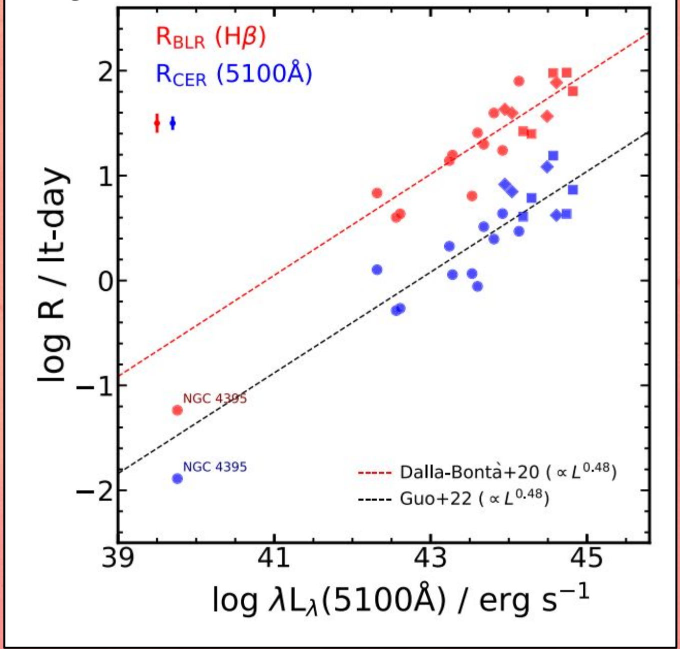

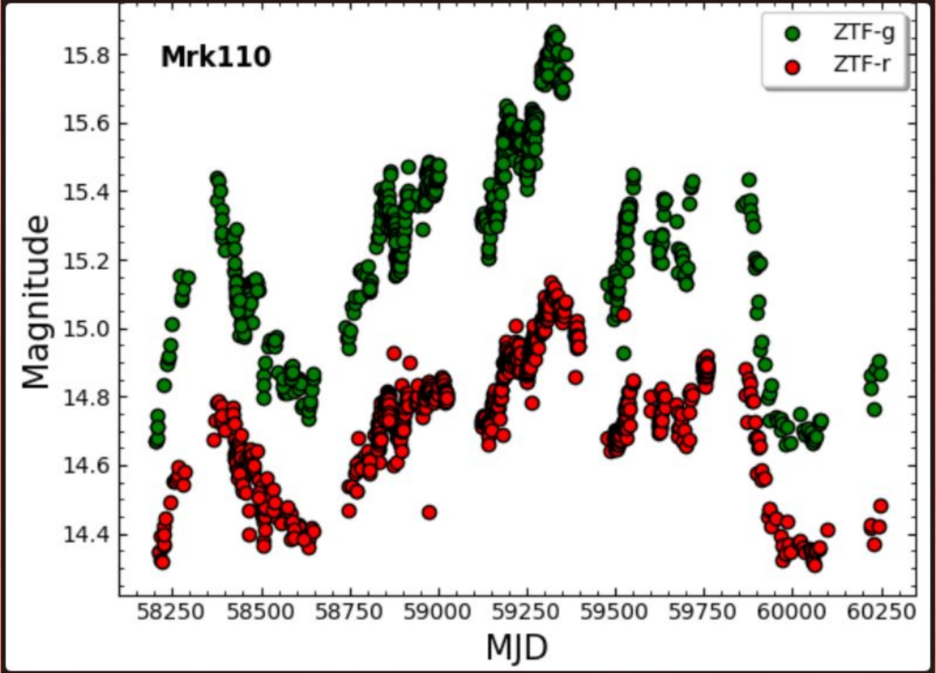

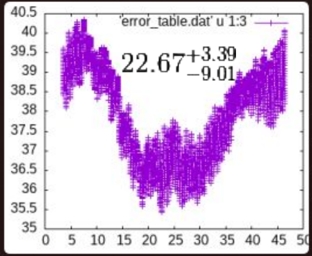

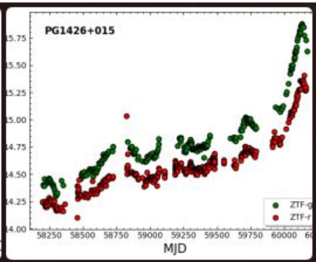

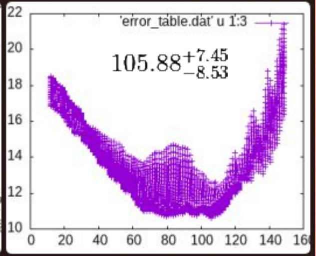

Real light curves from ZTF - testing with bonafide RM AGNs

SP, Czerny & Pozo-Nuñez (in prep.)

Wang et al. (2023)

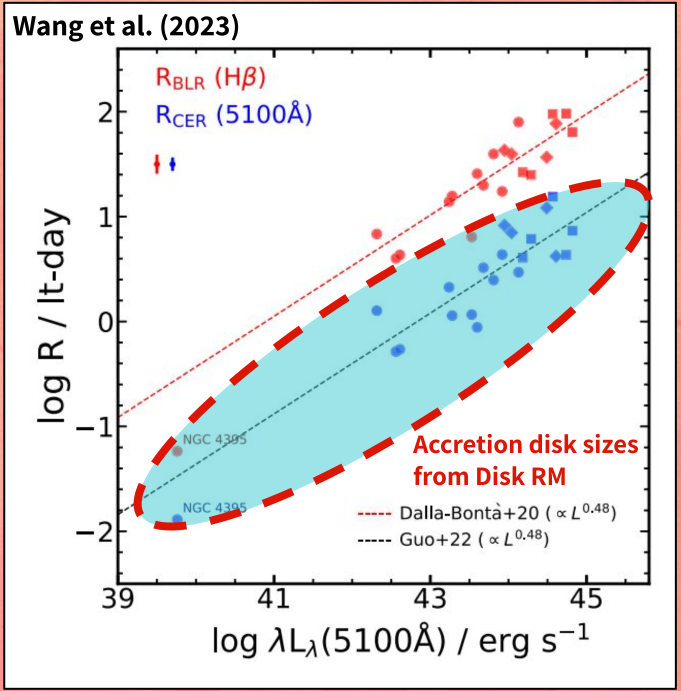

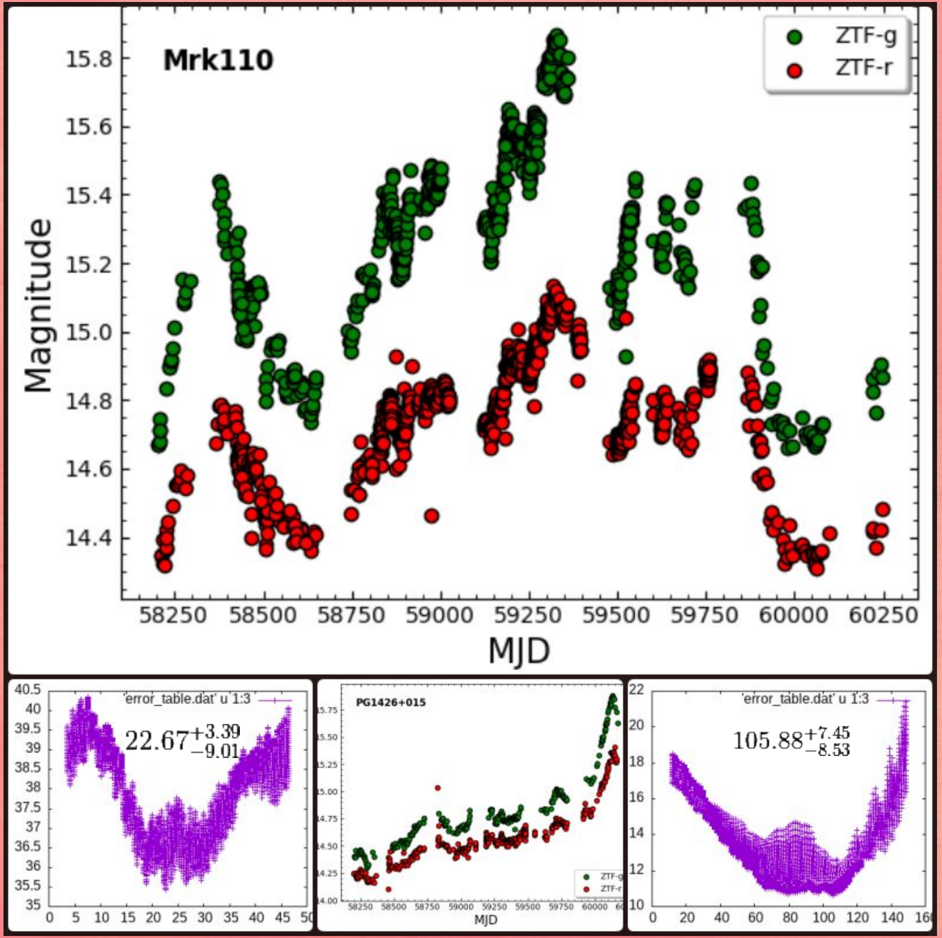

In progress

probabilistic cross-correlation approach using gaussian processes and model selection via cross validation

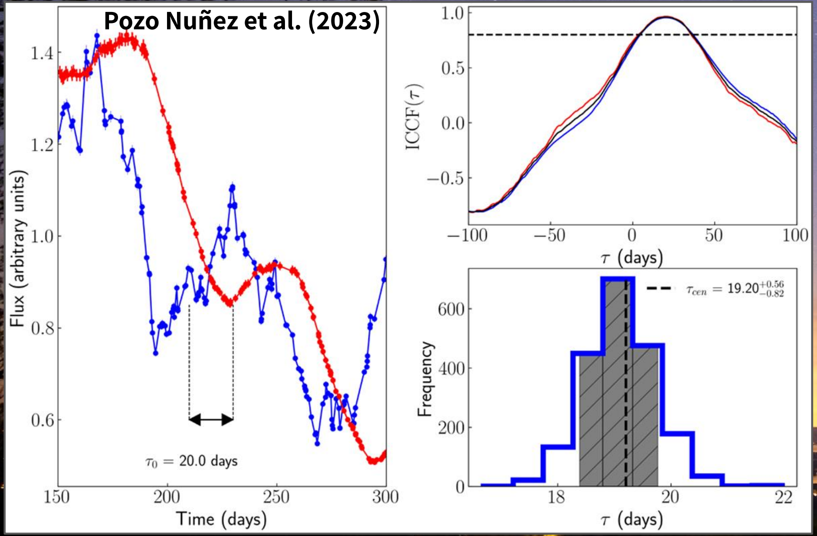

- *Improving the program to consistently generate the light-curves for all 6 photometric bands, with instrument delays.*
- *Efficient analyses accounting for the **contamination** from the starlight and other emission lines*
- ***Mock catalog** of light curves (1 deg^2 of the night sky will account for ~1000-4000 quasars): to produce artificial photometric light curves for each quasar*
- *Retrieving the expected number of quasars per square degree as a function of **redshift** and the **quasar magnitudes***
- *Improving the **prediction quality**, testing on the DDF fields*
- *Study of **break frequencies, PSD** distribution*
- *At present using the χ^2 method for **time delay estimation**, test and compare other methods:*
    - *ICCF, DCF, zDCF, JAVELIN, von-Neumann, & Bartels methods*

including the successful implementation of our code in a series of works)

Re-evaluating LSST survey strategies for optimal recovery of AGN properties across redshifts (esp. In the DDFs)

SP, Pozo-Nuñez, Czerny et al. (2024)

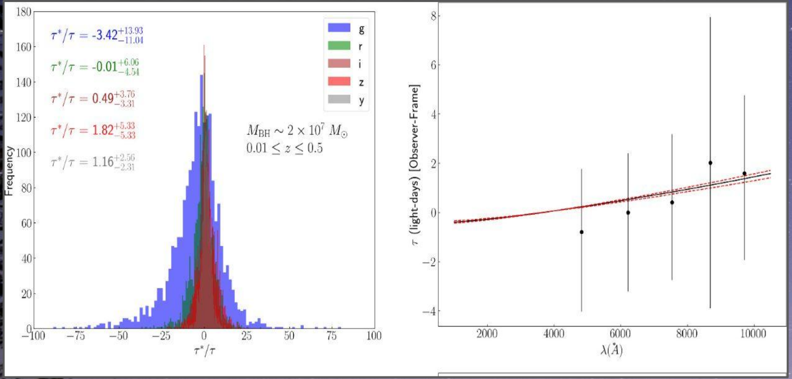

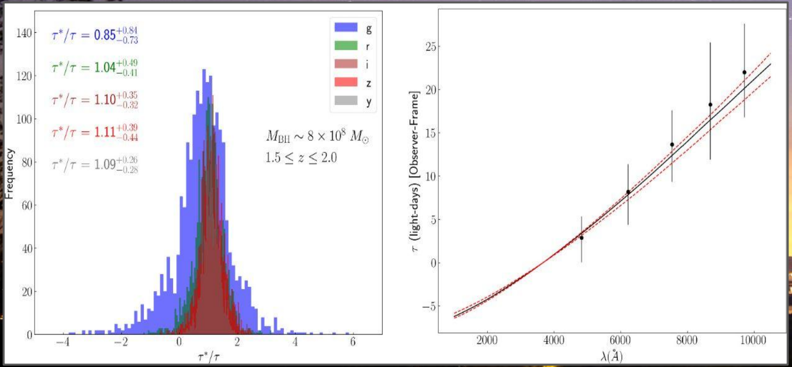

- *Improving the program to consistently generate the light-curves for all 6 photometric bands, with instrument delays.*
- *Efficient analyses accounting for the **contamination** from the starlight and other emission lines* ✅
- ***Mock catalog** of light curves (1 deg^2 of the night sky will account for ~1000-4000 quasars): to produce artificial photometric light curves for each quasar*
- *Retrieving the expected number of quasars per square degree as a function of **redshift** and the **quasar magnitudes***
- *Improving the **prediction quality**, testing on the DDF fields* ✅
- *Study of **break frequencies, PSD** distribution*
- *At present using the χ^2 method for **time delay estimation**, test and compare other methods:*
    - *ICCF, DCF, zDCF, JAVELIN, von-Neumann, & Bartels methods* ✅

  including the successful implementation of our code in a series of works)

Advantages of Continuum Reverberation Mapping

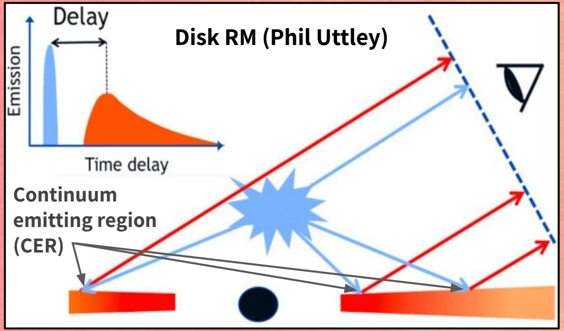

1. **AGN variability can be studied:**
    a. Either by quantifying the changes in the emission line variations (i.e, BLR) relative to the AGN continuum
    b. **Characterizing the variations in the AGN continuum**

Advantages of Continuum Reverberation Mapping

1. **AGN variability can be studied:**
   a. Either by quantifying the changes in the emission line variations (i.e, BLR) relative to the AGN continuum
   b. **Characterizing the variations in the AGN continuum**

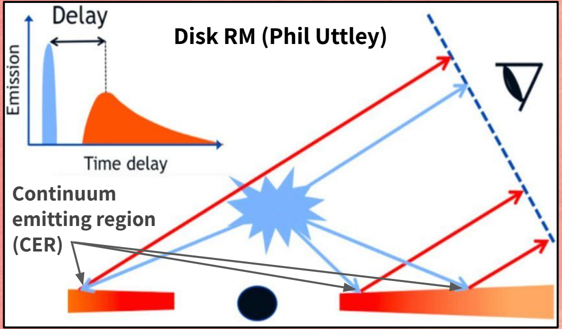

~40 nights monitoring of Mrk279 (z=0.03) → **disk lag of ~2.5 days**.

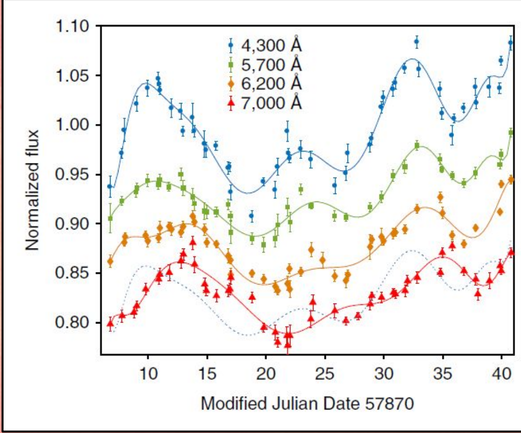

Chelouche et al. (2018)

BLR scattering is also important!

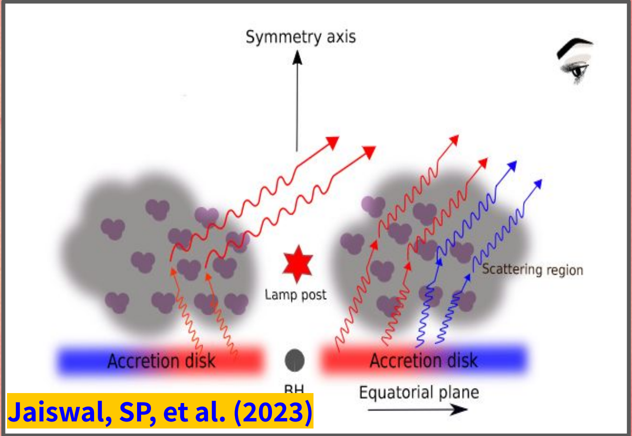

Jaiswal, SP, et al. (2023)

Aka Diffused continuum emission (DCE)

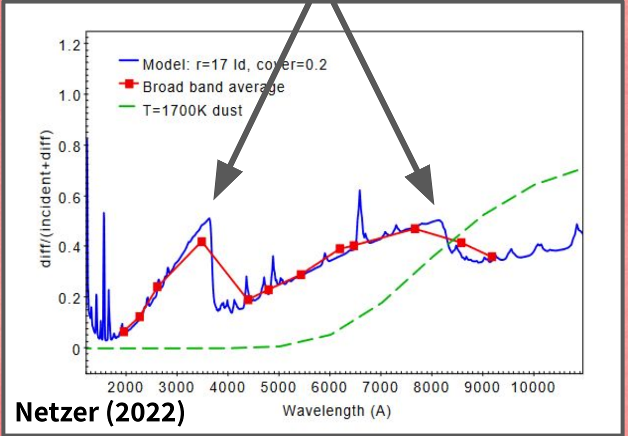

Netzer (2022)

Pozo-Nuñez, SP, et al. (2023)

AD Predictions for LSST: BLR contribution & time-sampling

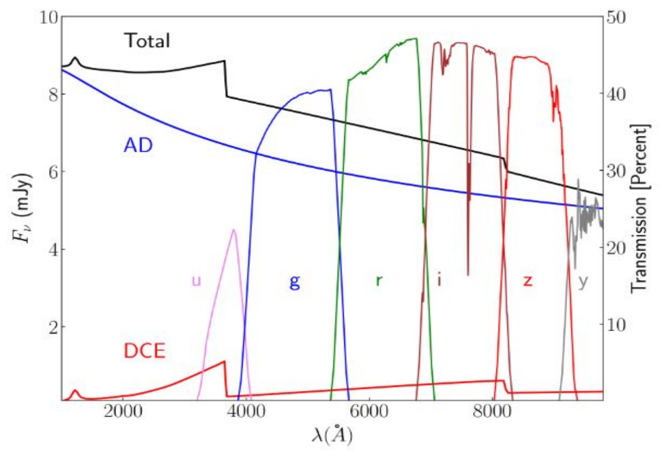

Figure 4. DCE and AD models for an arbitrary quasar obtained with the same model parameters as shown in Figure A1. The LSST transmission curves (*ugrizy*) are convolved with the quantum efficiency of the CCD camera and denoted by colored solid lines.

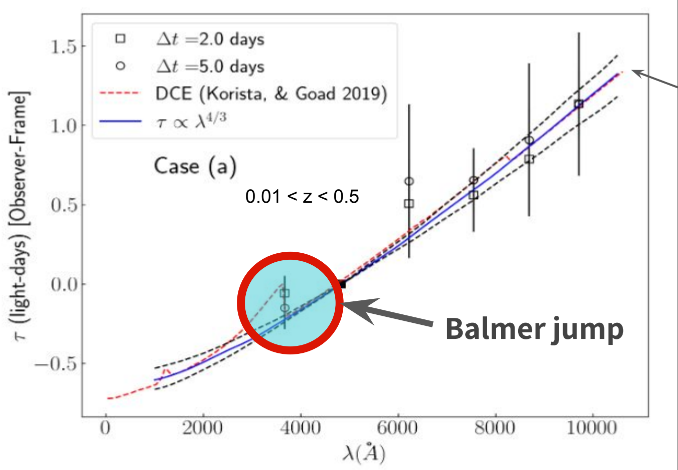

Figure 6. Same as Figure 5, but for Case(a) and an AD time delay spectrum recovered from observations with variable DCE from the BLR (red dotted line). The results are shown for a time sampling $\Delta t = 2$ days (filled squares).

The dotted lines show the delay spectrum obtained for a black hole mass with 30% uncertainty.

A minimum signal-to-noise ratio (S/N) of 100 with a BLR emission line contribution of less than 10% in the bandpasses can lead to recovery of the time delays with 5 and 10% accuracy for a time sampling of 2 and 5 days, respectively, and for quasars at 1.5 < z < 2.0

An accuracy of 10 to 20% can be achieved for quasars at z < 1.5 only if the contribution of the BLR emission lines is less than 5%.

Increasing the S/N does not improve the results significantly. Increased time sampling and reduced BLR emission line contamination is the solution to improve time delay accuracy.

Panda et al. (2024, ApJ Letters accepted)

A New Scaling relation (~150 times faster and more efficient!)

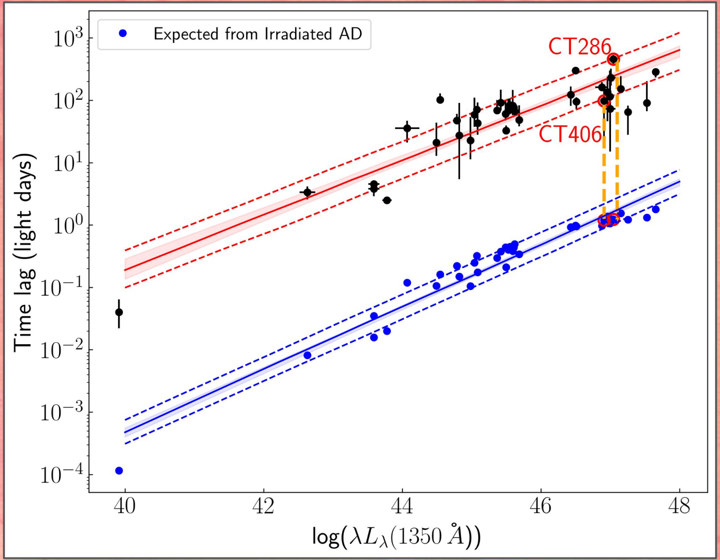

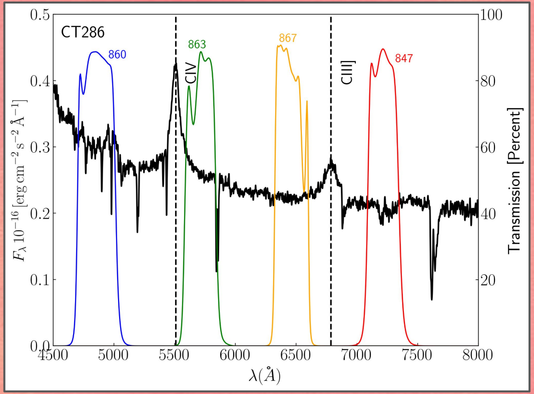

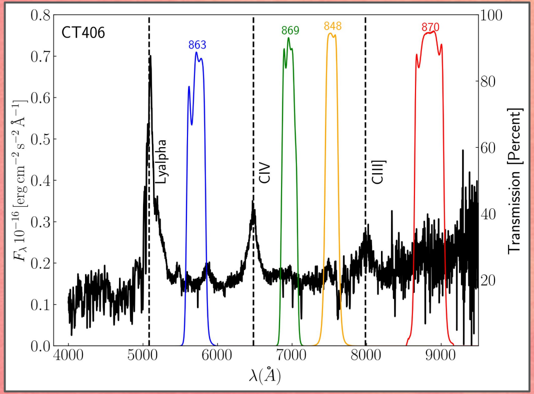

The La Silla 2.2m MPG/ESO telescope equipped with the Wide Field Imager camera with over 40 filters covering 3400-9600 Å.

- **CT286**, z=2.556, log L(1350Å) = 47.05 (~4 mins on target exposure)
- **CT406**, z=3.178, log L(1350Å) = 46.91 (~14 mins on target exposure)

Hβ RM usually takes ~100 to few hundred days even for the most luminous AGNs. While, the **CIV-based RM takes ~10-20 years** of monitoring.

The most up-to-date compilation of CIV RM AGNs was presented in Kaspi et al. (2021) with 38 AGNs where **0.001 < z < 3.4** and **39.9 < log L(1350Å) < 47.7**.

Panda et al. (2024, ApJ Letters accepted)

A New Scaling relation (~150 times faster and more efficient!)

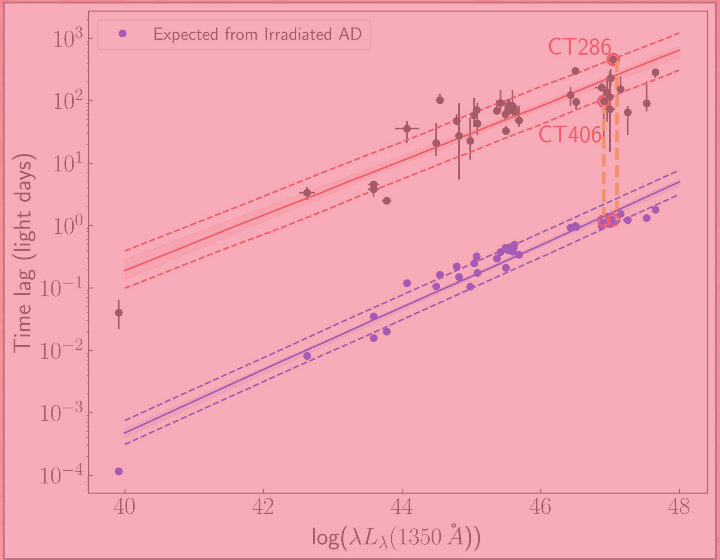

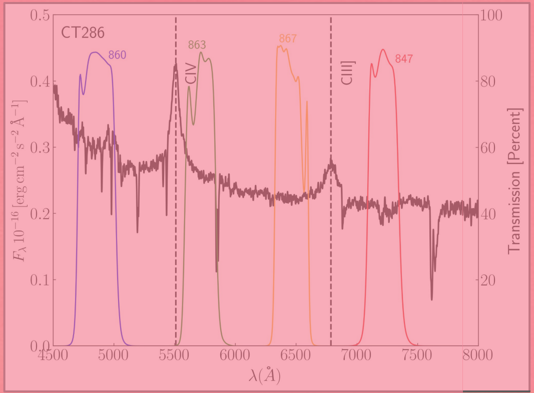

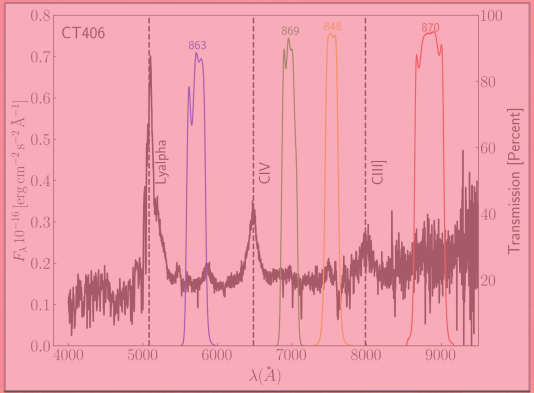

The La Silla 2.2m MPG/ESO telescope equipped with the Wide Field Imager camera with over 40 filters covering 3400-9600 Å.

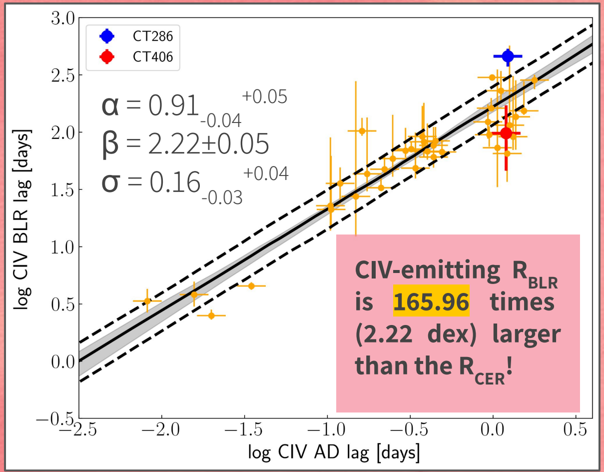

Hβ RM usually takes ~100 to few hundred days even for the most luminous AGNs. While, the **CIV-based**

Thank you for your attention!

presented in Kaspi et al. (2021) with 38 AGNs where **0.001 < z < 3.4** and **39.9 < log L(1350Å) < 47.7**.

= 46.91 (~14 mins on target exposure)

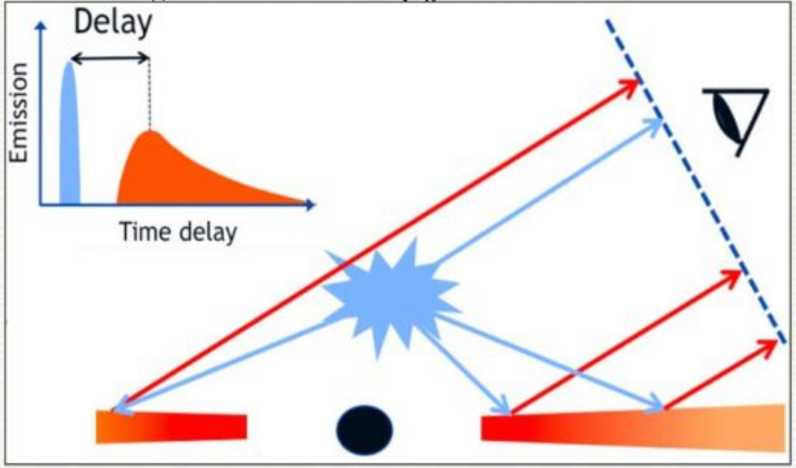

Courtesy: Phil Uttley

$$\tau = \tau_0 \left[(\lambda/\lambda_0)^{\beta} - 1 \right]$$

β ~ 1, much shallower

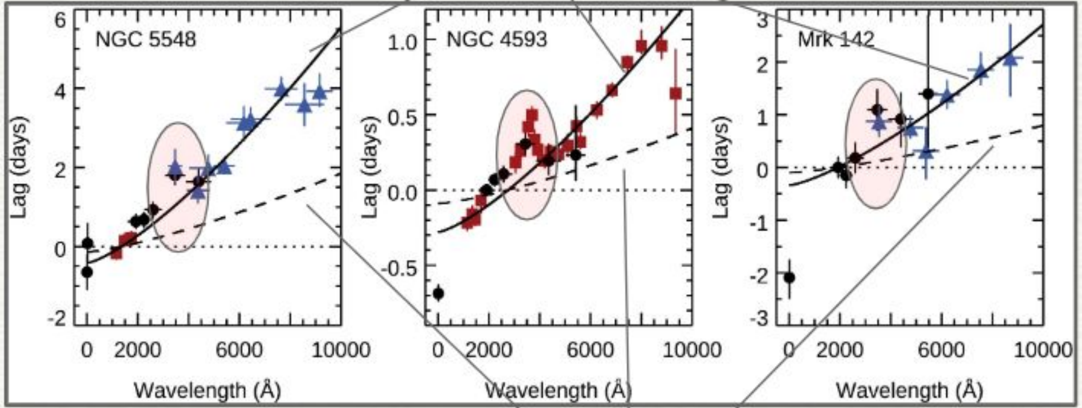

Cackett et al. (2021)

Standard Accretion disk predictions
$\beta = 4/3$

Accretion disk continuum lags modelling and predictions

$\tau_0^{predicted} \sim$ 2-3 $\tau_0^{standard\ disk}$

accretion disk size problem